

# X-Type Antiferromagnets

Shui-Sen Zhang,<sup>1,2,3</sup> Zi-An Wang,<sup>3,2</sup> Bo Li,<sup>4</sup> Shu-Hui Zhang,<sup>5</sup> Rui-Chun Xiao,<sup>6</sup> Lan-Xin Liu,<sup>3,2</sup> X. Luo,<sup>3</sup> W. J. Lu,<sup>3</sup>  
Mingliang Tian,<sup>1,7</sup> Y. P. Sun,<sup>1,3,8</sup> Evgeny Y. Tsymbal,<sup>9,\*</sup> Haifeng Du,<sup>1,6,†</sup> and Ding-Fu Shao<sup>3,‡</sup>

<sup>1</sup> *The Anhui Key Laboratory of Condensed Matter Physics at Extreme Conditions, High Magnetic Field Laboratory, Hefei Institutes of Physical Science, Chinese Academy of Sciences, Hefei 230031, China*

<sup>2</sup> *University of Science and Technology of China, Hefei 230026, China*

<sup>3</sup> *Key Laboratory of Materials Physics, Institute of Solid State Physics, Hefei Institutes of Physical Science, Chinese Academy of Sciences, Hefei 230031, China*

<sup>4</sup> *Institute for Advanced Study, Tsinghua University, Beijing, 100084, China*

<sup>5</sup> *College of Mathematics and Physics, Beijing University of Chemical Technology, Beijing 100029, People's Republic of China*

<sup>6</sup> *Institute of Physical Science and Information Technology, Anhui University, Hefei 230601, China*

<sup>7</sup> *School of Physics and Materials Science, Anhui University, Hefei 230601, China*

<sup>8</sup> *Collaborative Innovation Center of Microstructures, Nanjing University, Nanjing 210093, China*

<sup>9</sup> *Department of Physics and Astronomy & Nebraska Center for Materials and Nanoscience, University of Nebraska, Lincoln, Nebraska 68588-0299, USA*

Magnetically ordered materials reveal various types of magnetic moment alignment that affects their functional properties. This makes the exploration of unconventional magnetic orderings promising for the discovery of new physical phenomena and spintronic applications. Here, we introduce cross-chain antiferromagnets, dubbed X-type antiferromagnets, as an uncharted class of magnetically ordered crystals, where the stacking of two magnetic sublattices form an orthogonal pattern of intersecting atomic chains. These largely unexplored X-type antiferromagnets reveal unique spin-dependent transport properties that are not present in conventional magnets. Using  $\beta$ -Fe<sub>2</sub>PO<sub>5</sub> as a representative example of such X-type antiferromagnets, we predict the emergence of sublattice-selective spin-polarized transport, where one magnetic sublattice is conducting, while the other is not. As a result, spin torque can be exerted solely on a single sublattice, leading to unconventional ultrafast dynamics of the Néel vector capable of deterministic switching of the antiferromagnetic domains. Our work uncovers a previously overlooked type of magnetic moment alignment in antiferromagnets and reveals sublattice-selective physical properties promising for high-performance spintronic applications.

The alignment of magnetic moments in magnetically ordered materials determines their physical properties. For example, ferromagnets have parallel-aligned magnetic moments producing net magnetization that can be controlled by an applied magnetic field and is responsible for various spin-dependent transport properties. In contrast, antiferromagnets have magnetic orderings with atomic moments compensating each other and resulting in zero net magnetization [1, 2]. This property of antiferromagnets seems to be indicative of their spin-independent nature, not much promising for applications [3].

Despite this seemingly limiting constraint, antiferromagnets belong to a broad material family exhibiting diverse physical properties, some being technologically relevant. For example, antiferromagnets can produce an exchange bias on an adjacent ferromagnet [4, 5]. This property appeared to be practical for pinning the reference ferromagnetic (FM) layer in spin-valve read heads and magnetic random-access memories (MRAMs) that utilize tunneling magnetoresistance (TMR) effect. Antiferromagnetic (AFM) insulators with broken inversion symmetry, such as Cr<sub>2</sub>O<sub>3</sub>, are magnetoelectric [6, 7]. This

property has aroused significant interest in the past decade due to the possibility to control magnetic properties by electric fields. A plethora of interesting and potentially useful properties of antiferromagnets has been discovered recently. Among them are room-temperature anisotropic magnetoresistance [8], magnetic proximity effects [9], hidden [10, 11] and momentum-dependent [12–20] spin polarizations, spin currents, spin torques, and TMR effects [20–33]. These functional properties make antiferromagnets potentially useful for high-performance spintronic applications [34, 35].

Similar to ferromagnets and antiferromagnets being distinguished by their magnetic moment alignments, collinear antiferromagnets on their own are distinguished by different types of the AFM order. In general, an antiferromagnet is a magnetically-ordered crystal characterized by three attributes: 1) equal magnitudes of magnetization of magnetic sublattices,  $|\mathbf{m}_\alpha| = |\mathbf{m}_\beta|$ , where  $\alpha$  and  $\beta$  are sublattice indices; 2) vanishing net magnetization,  $\mathbf{M} \propto \sum_\alpha \mathbf{m}_\alpha = 0$ ; and 3) a long-range AFM order, corresponding to a Heisenberg model with

energy  $H = -\sum_{\alpha \neq \beta} J_{\alpha\beta} \mathbf{m}_\alpha \mathbf{m}_\beta$  and a negative exchange parameter  $J_{\alpha\beta} < 0$  between different sublattices. Figures 1a-1c illustrate typical G-, A-, and C-types of AFM alignments for simple cubic systems. For a G-type antiferromagnet, basic “building blocks” are isolated magnetic moments aligned antiparallel between all nearest neighbors (Fig. 1a). In this sense, a G-type antiferromagnet can be considered as “genuine,” due to AFM coupling solely controlling this type of ordering with FM coupling playing a secondary role. On the contrary, for A-type or C-type antiferromagnets, where the building blocks are antiparallel-aligned two-dimensional (2D) FM-ordered layers (Fig. 1b) or one-dimensional (1D) FM-ordered atomic chains (Fig. 1c), FM exchange interactions control the magnetic order in the 2D or 1D magnetic sublattices. Other known types of collinear AFM ordering involve D-, E-, and F-types of AFM alignments [36], which represent mixtures of parallel and orthogonal FM-aligned chains (D and F) combined with isolated magnetic moments antiparallel to all their nearest neighbors (E).

As we discussed in our recent paper [33], some AFM crystals exhibiting a C-type AFM order, e.g., those which belong to the rutile family, have small intra-sublattice distances resulting in strong intra-sublattice electron hopping between neighboring sites. A similar property is expected for certain A-type antiferromagnets. Therefore, from the electronic transport perspective, such A-type and C-type antiferromagnets qualitatively represent FM-ordered sublattices electrically connected in parallel. They support staggered Néel spin currents capable of driving spin-transfer torques and sizable TMR effects if used as electrodes in AFM tunnel junctions [33].

Even more exciting spin-dependent transport phenomena are expected for the antiferromagnets we introduce in this paper. These antiferromagnets represent 1D FM-ordered chains of atoms with opposite magnetic moment orientations (denoted as  $FM_A$  and  $FM_B$ ) as the basic building blocks of such antiferromagnets. Instead of alternating  $FM_A$  and  $FM_B$  chains parallel and to each other as in the C-type alignment, these antiferromagnets are composed of alternating layers of  $FM_A$  and  $FM_B$  chains parallel to each other within the plane but perpendicular between the adjacent layers (Fig. 1c). Unlike the A-type antiferromagnets with a similar FM ordering within the alternating planes, these antiferromagnets have a sizable separation between the chains making them rather isolated in each plane. This new type of AFM alignment does not violate the three above-mentioned attributes of the AFM order and thus should exist in nature. Due to  $FM_A$  and  $FM_B$  chain crossings in such antiferromagnets, we dub them as *cross-chain* antiferromagnets, or *X-type* antiferromagnets for short.

X-type antiferromagnets are expected to reveal unconventional transport properties never discovered before. Due to the pronounced anisotropy associated with the two orthogonal chain sublattices, X-type AFM metals are anticipated

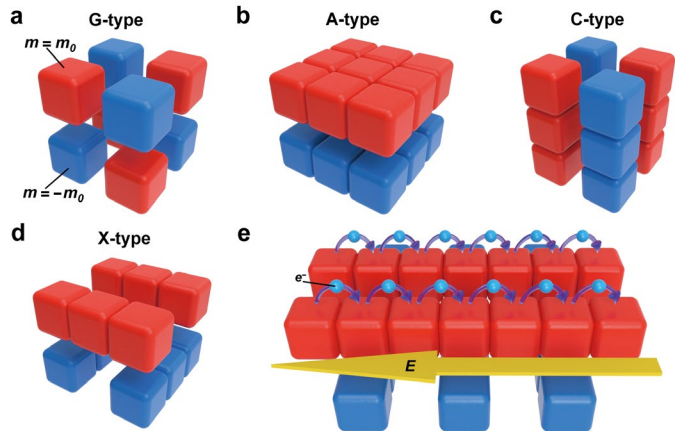


**Fig. 1: “Building blocks” for antiferromagnets.** **a.** A G-type antiferromagnet composed of isolated magnetic moments aligned antiparallel between all nearest neighbors. **b.** An A-type antiferromagnet composed of antiparallel-aligned FM layers. **c.** A C-type antiferromagnet composed of antiparallel-aligned FM chains. **d.** An X-type antiferromagnet composed of alternating layers of FM chains parallel to each other within the plane but perpendicular between the adjacent layers. **e.** The sublattice selective spin transport in an X-type antiferromagnet.

to exhibit strong anisotropy in their transport properties. For example, when applying an electric field along the  $FM_A$  direction, the  $FM_A$  chains are to be much more conductive for charge transport than the  $FM_B$  chains, provided by the strong intra-chain coupling and weak inter-chain coupling (Fig. 1e). In addition, due to the chains being FM-ordered, the current flowing along the  $FM_A$  chain must be spin-polarized. Therefore, unlike A-type and C-type antiferromagnets supporting staggered Néel spin currents on both sublattices, X-type antiferromagnets support isolated Néel spin currents selectively flowing along a single sublattice. Similarly, when applying an electric field along the  $FM_B$  direction, oppositely spin-polarized Néel spin currents appear in the  $FM_B$  chains, while the  $FM_A$  chains become non-conducting.

Driven by these expectations, in this paper, we explore electronic and spin-dependent transport properties of X-type antiferromagnets using density functional theory (DFT) and quantum-transport calculations by considering the AFM metal  $\beta$ - $Fe_2PO_5$  as a representative example. We demonstrate that X-type antiferromagnets support sublattice-selective spin-dependent transport, where for a selected transport direction, one magnetic sublattice is conducting, while the other is not. As a result of this unique property, spin torque can be exerted solely on a single sublattice, leading to unconventional ultrafast dynamics of the Néel vector capable of deterministic switching of AFM domains.

The collinear antiferromagnet  $\beta\text{-Fe}_2\text{PO}_5$  has been discovered more than 30 years ago [37] but remains not widely known. Figure 2a shows the crystal and magnetic structures of  $\beta\text{-Fe}_2\text{PO}_5$ , where the Fe atoms with upward and downward magnetic moments represent two magnetic sublattices denoted as  $\text{Fe}_A$  and  $\text{Fe}_B$ , respectively. The atomic structure of  $\beta\text{-Fe}_2\text{PO}_5$  contains in-plane chains of face-sharing  $\text{FeO}_6$  octahedra along the [100] and [010] directions of the tetragonal cell, which can be transformed to each other by a combined  $\hat{T}\hat{C}_{4z}$  symmetry operation, where  $\hat{T}$  is time reversal and  $\hat{C}_{4z}$  is a four-fold rotation around the  $z$  axis. The P atoms are located between these chains. The Fe ions have a mixed  $2+/3+$  valence and a small Fe-Fe intra-chain distance, favoring an intra-chain FM coupling via the double-exchange interaction [38]. These intersecting chains share common corners of the  $\text{FeO}_6$  octahedra. The resulting Fe-O-Fe bond angle is  $\sim 125^\circ$ , leading to a super-exchange interaction that favors the inter-chain AFM coupling [39]. Such an AFM alignment with a [001] directional Néel vector belongs to the magnetic space group  $I4_1'/am'd$  and represents an X-type antiferromagnet introduced above. The uniqueness of this type of AFM ordering, metallicity of  $\beta\text{-Fe}_2\text{PO}_5$  and its Néel temperature  $T_N = 408$  K [37] well above the room temperature make this collinear antiferromagnet interesting both for fundamental studies and for realistic applications.

We perform first-principles DFT calculations to explore the electronic and transport properties of  $\beta\text{-Fe}_2\text{PO}_5$ . Figures 2b and 2c show the calculated nonrelativistic band structure and Fermi surface of  $\beta\text{-Fe}_2\text{PO}_5$  and reveal giant momentum-dependent spin splitting, which was suggested to support nontrivial topological nodal fermions [40]. The emergence of such spin splitting in antiferromagnets can be understood from the group theory [12-19] and follows from the absence of combined  $\hat{P}\hat{T}$  or  $\hat{U}\hat{t}$  symmetry operations, where  $\hat{P}$  is space inversion,  $\hat{U}$  is spin rotation, and  $\hat{t}$  is lattice translation. In case of collinear AFM ordering, these antiferromagnets sometimes are referred to as “altermagnets” [17,18].

To elucidate spin-dependent transport properties, we calculate the through-bond transmission  $T_{ij} = T_{ij}^\uparrow + T_{ij}^\downarrow$  and through-bond spin transmission  $T_{ij}^s = T_{ij}^\uparrow - T_{ij}^\downarrow$  for transport along the [010] direction, where  $\uparrow$  and  $\downarrow$  denote the two spin channels, and  $i$  and  $j$  are the atomic indices [41]. As is evident from Figures 3a and 3b, these quantities reflect the anticipated chain-selective transport: both  $T_{ij}$  and  $T_{ij}^s$  are dominated by the  $\text{Fe}_A\text{-Fe}_A$  intra-chain bonds. It is notable that  $T_{ij}^s$  are negative, i.e., the spin current is flowing in the opposite direction to the charge current. This is due to the double exchange interaction between  $\text{Fe}_A^{2+}$  and  $\text{Fe}_A^{3+}$  ions, which is mostly mediated by the hopping of electrons with the spins opposite to the  $\text{Fe}_A$  moments. As a result, the spin-down bands along the  $\Gamma\text{-Y}$  direction are highly dispersive (Fig. 2b), leading to the spin-down Fermi sheets

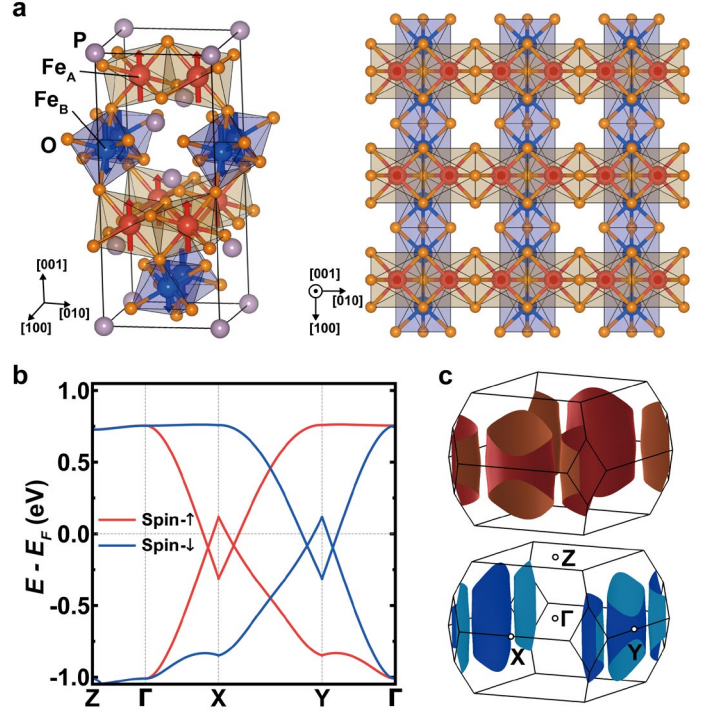


**Fig. 2: X-type antiferromagnet  $\beta\text{-Fe}_2\text{PO}_5$ .** *a. Left:* Crystal and magnetic structures of  $\beta\text{-Fe}_2\text{PO}_5$ . Arrows denote the magnetic moments of Fe atoms. *Right:* Top view of two bottom layers in the unit cell shown in the left. P atoms are ignored. *b.* Band structure of  $\beta\text{-Fe}_2\text{PO}_5$ . The Brillouin zone is shown in inset. *c.* The up-spin (top) and down-spin (bottom) Fermi surfaces of  $\beta\text{-Fe}_2\text{PO}_5$ .

representative to 1D transmission along the [010] direction (Fig. 2c). On the other hand, although there are mobile up-spin electrons on the  $\text{Fe}_B$  chains to mediate the intra-chain double-exchange interaction, the weak inter-chain coupling due to the large  $\text{Fe}_A\text{-Fe}_B$  and  $\text{Fe}_B\text{-Fe}_B$  inter-chain distances leads to negligible  $T_{ij}$  and  $T_{ij}^s$  associated with  $\text{Fe}_B$ . Therefore, the dispersions of the up-spin bands are weak and have a large energy gap in the  $\Gamma\text{-Y}$  direction (Fig. 2b). The transport spin polarization in this case is estimated to be as high as  $\sim 68\%$  in the ballistic regime, which is further enhanced to  $\sim 94\%$  in the diffusive regime, due to a small  $T_{ij}^{(s)}$  associated with  $\text{Fe}_B$  being scattered out [42]. Similarly, for transport along the [100] direction, the total transmission is majorly contributed by the hopping of spin-up electrons between intra-chain  $\text{Fe}_B$  atoms, corresponding to the band structure along the  $\Gamma\text{-X}$  direction and leading the spin-up Fermi surface sheets (Figs. 2b and 2c). Therefore, the spin-split electronic structure of  $\beta\text{-Fe}_2\text{PO}_5$  can be qualitatively considered as the superposition of the electronic structures of the isolated  $\text{Fe}_A$  and  $\text{Fe}_B$  chains.

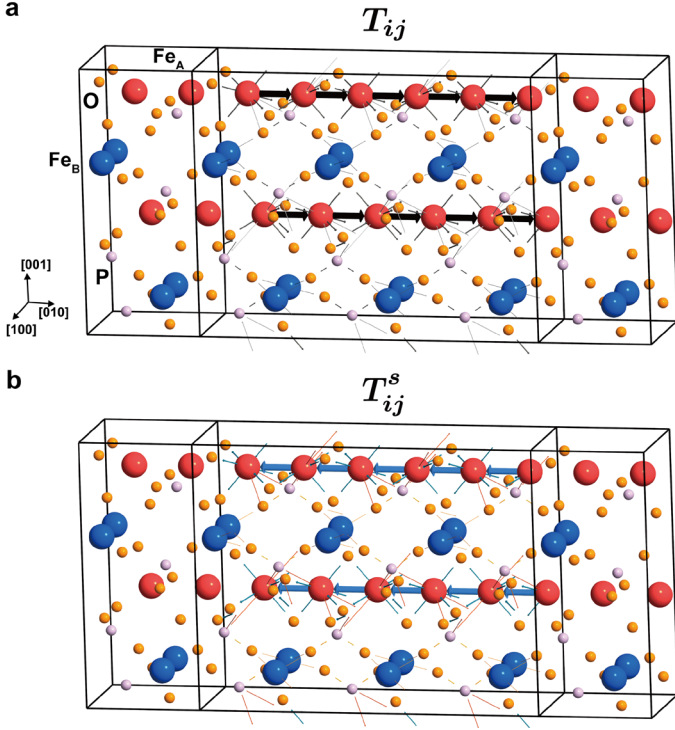


**Fig. 3: Sublattice-selective spin-dependent transport in X-type antiferromagnet  $\beta\text{-Fe}_2\text{PO}_5$ .** **a, b.** Visualization of the calculated through-bond transmissions  $T_{ij}$  (a) and through-bond spin transmissions  $T_{ij}^s$  (b) of  $\beta\text{-Fe}_2\text{PO}_5$ . The directions of arrows indicate sign of  $T_{ij}^{(s)}$  between atoms  $i$  and  $j$ , i.e. a rightward (leftward) arrow imply  $T_{ij}^{(s)}$  being positive (negative). The width of the arrows is proportional to  $\sqrt{|T_{ij}^{(s)}|}$ .

The strong intra-chain spin transmission supports highly spin-polarized Néel spin currents along the chains in  $\beta\text{-Fe}_2\text{PO}_5$ . These Néel spin currents are highly anisotropic due to the unique X-type AFM alignment. For example, an electric field along the  $[110]$  direction produces crossing Néel spin currents with opposite spin polarizations along the Fe<sub>A</sub> and Fe<sub>B</sub> chains. These currents can be decomposed into a transverse global spin current and the staggered longitudinal Néel spin current hidden in a globally spin-neutral current. On the other hand, when the electric field is along one of the chain directions ( $[100]$  or  $[010]$ ), only the longitudinal chains are conductive producing an isolated Néel spin current, while the transverse chains are almost insulating.

Usually, time-reversal-odd transport properties, such as spin currents, strongly depend on the net magnetization  $\mathbf{M}$  in magnetic materials. This is not the case for  $\beta\text{-Fe}_2\text{PO}_5$ . In  $\beta\text{-Fe}_2\text{PO}_5$ ,  $\mathbf{M}$  is controlled by the number of layers, i.e.,  $\mathbf{M}$  is vanishing for an even-layer  $\beta\text{-Fe}_2\text{PO}_5$  and is positive (negative)

for  $\beta\text{-Fe}_2\text{PO}_5$  with more Fe<sub>A</sub> (Fe<sub>B</sub>) layers. The high spin polarization of the longitudinal spin current in  $\beta\text{-Fe}_2\text{PO}_5$ , however, is not influenced by the number of layers, since it is contributed solely by the isolated Néel spin currents on selected sublattices. Such a sublattice selective spin-dependent transport property is very interesting, as it opens a possibility to realize the sublattice-resolved spintronic phenomena.

As an example, we show that X-type antiferromagnets allow exerting a spin torque on a single magnetic sublattice. This can be achieved by passing an external spin current along one of the FM-chain directions or by using an isolated Néel spin current on one type of FM chains in the presence of asymmetric boundary conditions to generate self-torque. Assuming that the current is flowing along the FM<sub>A</sub> sublattice with magnetic moments  $\mathbf{m}_A$  pointing to the  $+z$  direction, the associated magnetic dynamics of an X-type antiferromagnet can be described by the Landau-Lifshitz-Gilbert-Slonczewski equations [43,44]:

$$\begin{aligned}\dot{\mathbf{m}}_A &= \boldsymbol{\tau}_A^F + \boldsymbol{\tau}_A^D + \boldsymbol{\tau}_A^{FL} + \boldsymbol{\tau}_A^{DL}, \\ \dot{\mathbf{m}}_B &= \boldsymbol{\tau}_B^F + \boldsymbol{\tau}_B^D.\end{aligned}\quad (1)$$

Here  $\boldsymbol{\tau}_\alpha^F \propto -\mathbf{m}_\alpha \times \mathbf{H}_{eff,\alpha}$  and  $\boldsymbol{\tau}_\alpha^D \propto \mathbf{m}_\alpha \times \dot{\mathbf{m}}_\alpha = -\mathbf{m}_\alpha \times (\mathbf{m}_\alpha \times \mathbf{H}_{eff,\alpha})$  are the precession and damping torques on sublattice  $\alpha$  induced by the intrinsic effective field  $\mathbf{H}_{eff,\alpha}$ , respectively, and  $\boldsymbol{\tau}_A^{FL} \propto -\mathbf{m}_A \times \mathbf{H}_{st}$  and  $\boldsymbol{\tau}_A^{DL} \propto -\mathbf{m}_A \times (\mathbf{m}_A \times \mathbf{H}_{st})$  are the field-like and damping-like torques driven by a spin-torque effective field  $\mathbf{H}_{st}$  oriented toward the  $-z$  direction. Since  $\mathbf{H}_{eff,\alpha}$  includes the anisotropy field  $\mathbf{H}_{K,\alpha}$  and the exchange field  $\mathbf{H}_{E,\alpha}$ , the  $\boldsymbol{\tau}_\alpha^F$  and  $\boldsymbol{\tau}_\alpha^D$  can be further decomposed as  $\boldsymbol{\tau}_\alpha^F = \boldsymbol{\tau}_{K,\alpha}^F + \boldsymbol{\tau}_{E,\alpha}^F$  and  $\boldsymbol{\tau}_\alpha^D = \boldsymbol{\tau}_{K,\alpha}^D + \boldsymbol{\tau}_{E,\alpha}^D$ , where the subscripts  $K$  and  $E$  denote the associated torques driven by  $\mathbf{H}_{K,\alpha}$  and  $\mathbf{H}_{E,\alpha}$ , respectively. Due to  $\mathbf{H}_{E,\alpha}$  being much larger than  $\mathbf{H}_{K,\alpha}$ ,  $\boldsymbol{\tau}_\alpha^F \approx \boldsymbol{\tau}_{E,\alpha}^F$  and  $\boldsymbol{\tau}_\alpha^D \approx \boldsymbol{\tau}_{E,\alpha}^D$  when  $\mathbf{m}_A$  and  $\mathbf{m}_B$  are not perfectly antiparallel. Figures 4a and 4b schematically show how these torques affect the dynamics of  $\mathbf{m}_A$  and  $\mathbf{m}_B$ . When the isolated spin-torque carrying effective field  $\mathbf{H}_{st}$  is applied solely to  $\mathbf{m}_A$ , the associated damping-like torque  $\boldsymbol{\tau}_A^{DL}$  pulls  $\mathbf{m}_A$  away from the easy-axis toward the  $-z$  direction. This creates canting between  $\mathbf{m}_A$  and  $\mathbf{m}_B$ , and hence  $\mathbf{H}_{E,\alpha}$  exerts non-zero torques  $\boldsymbol{\tau}_\alpha^F$  and  $\boldsymbol{\tau}_\alpha^D$  on both moments  $\mathbf{m}_A$  and  $\mathbf{m}_B$ . The torque  $\boldsymbol{\tau}_\alpha^F$  generates oscillations of the Néel vector, while the torque  $\boldsymbol{\tau}_B^D$  pulls  $\mathbf{m}_B$  toward  $+z$  direction even without assistance of an external spin torque. Using realistic parameters  $\mathbf{H}_{K,\alpha} = 2$  T,  $\mathbf{H}_{E,\alpha} = 100$  T, and the damping factor of 0.01, we find that  $\mathbf{H}_{st}$  being much smaller than  $\mathbf{H}_{K,\alpha}$  ( $0.17|\mathbf{H}_{K,\alpha}| < |\mathbf{H}_{st}| < 0.24|\mathbf{H}_{K,\alpha}|$ ) is sufficient to switch the Néel vector (Fig. 4c). The switching trajectory is similar to that for the spin-transfer torque in ferromagnets [43-46], indicating the decisive role of the damping-like torque  $\boldsymbol{\tau}_A^{DL}$ . Since this  $\mathbf{H}_{st}$  can be driven by an external spin current, the AFM domains can be aligned according to the spin polarization of the external spin source.



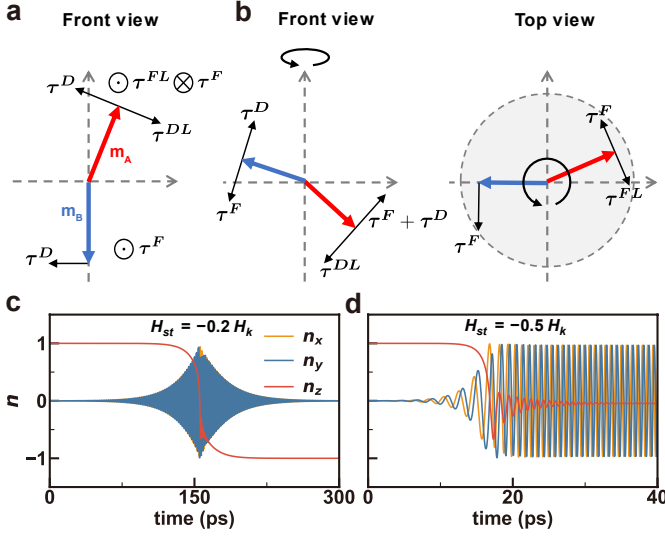


**Fig. 4: Sublattice selective spin torques in X-type antiferromagnet.** **a.** Vectors of magnetic moments and spin torques in the initial spin dynamics. **b.** Vectors of magnetic moments and spin torques in the process of Néel vector oscillations driven by the single-sublattice spin torque: front (left) and top (right) views. **c,d.** Simulated dynamics of the  $x$ ,  $y$ , and  $z$  components of the normalized Néel vector  $\mathbf{n}$  under the current-induced spin-torque effective field  $H_{st} = -0.2H_K$  (c) and  $H_{st} = -0.5H_K$  (d).

This solves the challenging problem of AFM spintronics where measurable time-reversal-odd properties (e.g., TMR in AFM tunnel junctions) are strongly diminished by misaligned domains.

Interestingly, we find that a larger  $H_{st}$  ( $|H_{st}| > 0.24|H_{K,\alpha}|$ ) can drive ultrafast oscillations of the Néel vector (Fig. 4d). This is because of the much stronger canting of  $\mathbf{m}_A$  and  $\mathbf{m}_B$  that produces a large out-of-plane component of  $\boldsymbol{\tau}_A^f$  competing with  $\boldsymbol{\tau}_A^{DL}$ . This property distinguishes the dynamics of X-type antiferromagnets from other antiferromagnets, where full switching and ultrafast oscillations cannot be generated using the same type of spin torques [25,27,47].

The X-type AFM alignment is expected to emerge in materials other than  $\beta\text{-Fe}_2\text{PO}_5$ . 3d transition metal atoms, such as V, Ni, and Cr, can be used to replace Fe in  $\beta\text{-Fe}_2\text{PO}_5$  to form the cross-chain structure [48-50]. One can engineer the spin states of these compounds by controlling the amount of doping for a desirable exchange interaction. It would also be interesting to achieve the X-type AFM alignment in other crystalline systems, for example, in hexagonal antiferromagnets, where the opposite

chains are not aligned perpendicular but have a non-zero angle between each other. In addition, modern film-growth techniques allow layer-by-layer deposition of thin films. Therefore, one can envision an atomic scale superlattice of  $[L_2\text{PO}_5/M_2\text{PO}_5]$  ( $L$  and  $M$  are different magnetic atoms), which may form *cross-chain ferrimagnets* with the X-type magnetic ordering and sublattice-selective spin-transport properties.

From the technological point of view, X-type antiferromagnets offer a new approach for non-volatile memories. For example, in a single-domain X-type antiferromagnet, one can selectively reverse domains by passing an isolated Néel spin current or an external spin current along the chosen  $\text{FM}_A$  or  $\text{FM}_B$  chains. This promises an ultrafast AFM racetrack memory, where the opposite AFM domains can serve as “0” and “1” bits of information. Moreover, the X-type AFM alignment with crossing chains of magnetic atoms forms an intrinsic crossbar array that is widely used in MRAMs, which may be exploited in future big-data applications.

Overall, X-type antiferromagnets signify an exciting field of research for fundamental science and an attractive new paradigm for AFM spintronics. The predicted sublattice-selective electronic transport carrying isolated Néel spin currents has multiple important implications, such as spin torques exerted on a single magnetic sublattice, unconventional ultrafast spin dynamics, and deterministic switching of the AFM domains. These unprecedented functionalities promise new AFM spintronic devices which can be employed in non-volatile memories with ultra-high density and ultra-fast switching speed. We hope therefore that our theoretical results will stimulate the experimentalists working in this field to explore the predicted properties of X-type antiferromagnets relevant to spintronics and beyond.

**Acknowledgments.** This work was supported by the National Key R&D Program of China (Grant No. 2021YFA1600200), the National Natural Science Foundation of China (Grants Nos. 12274411, 12241405, and 52250418), and the CAS Project for Young Scientists in Basic Research No. YSBR-084. E.Y.T acknowledges support from the Division of Materials Research of the National Science Foundation (NSF grant No. DMR-2316665). Computations were performed at Hefei Advanced Computing Center.

\* [tsymbal@unl.edu](mailto:tsymbal@unl.edu)  
† [duhf@hmfl.ac.cn](mailto:duhf@hmfl.ac.cn)  
‡ [dfshao@issp.ac.cn](mailto:dfshao@issp.ac.cn)

[1] L. Néel, Propriétés magnétiques du manganèse et du chrome en solution solide étendue, *J. Phys. Radium* **3**, 160 (1932).

[2] L. Néel, Antiferromagnetism and Ferrimagnetism, *Proc. Phys. Soc. Sect. A* **65**, 869 (1952).

- [3] Nobel Lectures, Physics, 1963-1970: Including Presentation Speeches and Laureates' Biographies. Amsterdam: Elsevier Pub. Company for the Nobel Foundation (1972).
- [4] W. H. Meiklejohn and C. P. Bean, New magnetic anisotropy, *Phys. Rev.* **105**, 904 (1957).
- [5] J. Nogués and I. K. Schuller, Exchange bias, *J. Magn. Magn. Mater.* **192**, 203 (1999).
- [6] I. Dzyaloshinskii, On the magneto-electrical effect in antiferromagnets, *Sov. Phys. JETP* **10**, 628 (1960).
- [7] D. Astrov, The magnetoelectric effect in antiferromagnets, *Sov. Phys. JETP* **11**, 708 (1960).
- [8] X. Marti, I. Fina, C. Frontera, Jian Liu, P. Wadley, Q. He, R. J. Paull, J. D. Clarkson, J. Kudrnovský, I. Turek, J. Kuneš, D. Yi, J.-H. Chu, C. T. Nelson, L. You, E. Arenholz, S. Salahuddin, J. Fontcuberta, T. Jungwirth, and R. Ramesh, Room-temperature antiferromagnetic memory resistor, *Nat. Mater.* **3**, 367–374 (2014).
- [9] T. S. Ghiasi, A. A. Kaverzin, A. H. Dismukes, D. K. de Wal, X. Roy, and B. J. van Wees, Electrical and thermal generation of spin currents by magnetic bilayer graphene, *Nat. Nanotechnol.* **16**, 788 (2021).
- [10] X. Zhang, Q. Liu, J.-W. Luo, A. J. Freeman, and A. Zunger, Hidden spin polarization in inversion-symmetric bulk crystals, *Nat. Phys.* **10**, 387 (2014).
- [11] L.-D. Yuan, X. Zhang, C. M. Acosta, and A. Zunger, Uncovering spin-orbit coupling-independent hidden spin polarization of energy bands in antiferromagnets, *Nat. Commun.* **14**, 5301 (2023).
- [12] S. Hayami, Y. Yanagi, and H. Kusunose, Momentum-dependent spin splitting by collinear antiferromagnetic ordering, *J. Phys. Soc. Jpn.* **88**, 123702 (2019).
- [13] L.-D. Yuan, Z. Wang, J.-W. Luo, E. I. Rashba, and A. Zunger, Giant momentum-dependent spin splitting in centrosymmetric low-Z antiferromagnets, *Phys. Rev. B* **102**, 014422 (2020).
- [14] L.-D. Yuan, Z. Wang, J.-W. Luo, and A. Zunger, A. Prediction of low-Z collinear and noncollinear antiferromagnetic compounds having momentum-dependent spin splitting even without spin-orbit coupling, *Phys. Rev. Mater.* **5**, 014409 (2021).
- [15] S. Hayami, Y. Yanagi, and H. Kusunose, Bottom-up design of spin-split and reshaped electronic band structures in antiferromagnets without spin-orbit coupling: Procedure on the basis of augmented multipoles, *Phys. Rev. B* **102**, 144441 (2020).
- [16] P. Liu, J. Li, J. Han, X. Wan, and Q. Liu, Spin-group symmetry in magnetic materials with negligible spin-orbit coupling, *Phys. Rev. X* **12**, 021016 (2022).
- [17] L. Šmejkal, J. Sinova, and T. Jungwirth, Beyond Conventional Ferromagnetism and Antiferromagnetism: A Phase with Nonrelativistic Spin and Crystal Rotation Symmetry, *Phys. Rev. X* **12**, 031042 (2022).
- [18] L. Šmejkal, J. Sinova, and T. Jungwirth, Emerging Research Landscape of Altermagnetism, *Phys. Rev. X* **12**, 040501 (2022).
- [19] L. Yuan, A. Zunger, Degeneracy Removal of Spin Bands in Collinear Antiferromagnets with Non-Interconvertible Spin-Structure Motif Pair, *Adv. Mater.* **35**, 2211966 (2023).
- [20] J. Železný, Y. Zhang, C. Felser, and B. Yan, Spin-polarized current in noncollinear antiferromagnets, *Phys. Rev. Lett.* **119**, 187204 (2017).
- [21] M. Naka, S. Hayami, H. Kusunose, Y. Yanagi, Y. Motome, and H. Seo, Spin current generation in organic antiferromagnets, *Nat. Commun.* **10**, 4305 (2019).
- [22] R. González-Hernández, L. Šmejkal, K. Výborný, Y. Yahagi, J. Sinova, T. Jungwirth, and J. Železný, Efficient electrical spin-splitter based on non-relativistic collinear antiferromagnetism, *Phys. Rev. Lett.* **126**, 127701 (2021).
- [23] G. Gurung, D.-F. Shao, and E. Y. Tsymlal, Transport Spin Polarization of Noncollinear Antiferromagnetic Antiperovskites, *Phys. Rev. Mater.* **5**, 124411 (2021).
- [24] H. Y. Ma, M. Hu, N. Li, J. Liu, W. Yao, J.-F. Jia, and J. Liu, Multifunctional antiferromagnetic materials with giant piezomagnetism and noncollinear spin current, *Nat. Commun.* **12**, 2846 (2021).
- [25] J. Železný, H. Gao, K. Výborný, J. Zemen, J. Mašek, A. Manchon, J. Wunderlich, J. Sinova, and T. Jungwirth, Relativistic Néel-Order Fields Induced by Electrical Current in Antiferromagnets, *Phys. Rev. Lett.* **113**, 157201 (2014).
- [26] P. Wadley, B. Howells, J. Železný, C. Andrews, V. Hills, R. P. Campion, V. Novák, K. Olejník, F. Maccherozzi, S. S. Dhesi, S. Y. Martin, T. Wagner, J. Wunderlich, F. Freimuth, Y. Mokrousov, J. Kuneš, J. S. Chauhan, M. J. Grzybowski, A. W. Rushforth, K. W. Edmonds, B. L. Gallagher, and T. Jungwirth, Electrical switching of an antiferromagnet, *Science* **351**, 587 (2016).
- [27] A. Manchon, J. Železný, I. M. Miron, T. Jungwirth, J. Sinova, A. Thiaville, K. Garello, and P. Gambardella, Current-induced spin-orbit torques in ferromagnetic and antiferromagnetic systems, *Rev. Mod. Phys.* **91**, 035004 (2019).
- [28] D.-F. Shao, S. H. Zhang, M. Li, C. B. Eom, and E. Y. Tsymlal, Spin-neutral currents for spintronics, *Nat. Commun.* **12**, 7061 (2021).
- [29] L. Šmejkal, A. Birk Hellenes, R. González-Hernández, J. Sinova, and T. Jungwirth, Giant and tunneling magnetoresistance in unconventional collinear antiferromagnets with nonrelativistic spin-momentum coupling, *Phys. Rev. X* **12**, 011028 (2022).
- [30] J. Dong, X. Li, G. Gurung, M. Zhu, P. Zhang, F. Zheng, E. Y. Tsymlal, and J. Zhang, Tunneling magnetoresistance in noncollinear antiferromagnetic tunnel junctions, *Phys. Rev. Lett.* **128**, 197201 (2022).
- [31] P. Qin, H. Yan, X. Wang, H. Chen, Z. Meng, J. Dong, M. Zhu, J. Cai, Z. Feng, X. Zhou, L. Liu, T. Zhang, Z. Zeng, J. Zhang, C. Jiang, and Z. Liu, Room-temperature magnetoresistance in an all-antiferromagnetic tunnel junction, *Nature* **613**, 485 (2023).
- [32] X. Chen, T. Higo, K. Tanaka, T. Nomoto, H. Tsai, H. Idzuchi, M. Shiga, S. Sakamoto, R. Ando, H. Kosaki, T. Matsuo, D. Nishio-Hamane, R. Arita, S. Miwa, and S. Nakatsuji, Octupole-driven magnetoresistance in an antiferromagnetic tunnel junction, *Nature* **613**, 490 (2023).
- [33] D. F. Shao, Y. Y. Jiang, J. Ding, S. H. Zhang, Z. A. Wang, R. C. Xiao, G. Gurung, W. J. Lu, Y. P. Sun, and E. Y. Tsymlal, Neel Spin Currents in Antiferromagnets, *Phys. Rev. Lett.* **130**, 216702 (2023).
- [34] T. Jungwirth, X. Marti, P. Wadley, and J. Wunderlich, Antiferromagnetic spintronics, *Nat. Nanotechnol.* **11**, 231 (2016).
- [35] V. Baltz, A. Manchon, M. Tsoi, T. Moriyama, T. Ono, and Y. Tserkovnyak, Antiferromagnetic spintronics, *Rev. Mod. Phys.* **90**, 015005 (2018).
- [36] E. O. Wollan and W. C. Koehler, Neutron Diffraction Study of the Magnetic Properties of the Series of Perovskite-Type Compounds  $[(1-x)\text{La}, x\text{Ca}]\text{MnO}_3$ , *Phys. Rev.* **100**, 545 (1955).

- [37] M. Ijjaali, B. Malaman, C. Gleitzer, J. K. Warner, J. A. Hriljac, and A.K. Cheetham, Stability, structure refinement, and magnetic properties of  $\beta$ -Fe<sub>2</sub>(PO<sub>4</sub>)O, *J. Solid State Chem.* **86**, 195 (1990).
- [38] C. Zener, Interaction between the *d*-Shells in the Transition Metals. II. Ferromagnetic Compounds of Manganese with Perovskite Structure. *Phys. Rev.* **82**, 403–405 (1951).
- [39] P. W. Anderson, Antiferromagnetism. Theory of Superexchange Interaction. *Phys. Rev.* **79**, 350–356 (1950).
- [40] T. He, X. Zhang, W. Meng, L. Jin, X. Dai, and G. Liu, Topological nodal lines and nodal points in the antiferromagnetic material  $\beta$ -Fe<sub>2</sub>PO<sub>5</sub>, *J. Mater. Chem. C* **7**, 12657 (2019).
- [41] G. C. Solomon, C. Herrmann, T. Hansen, V. Mujica, and M. A. Ratner. Exploring local currents in molecular junctions. *Nat. Chem.* **2**, 223 (2010).
- [42] See Supplemental Material.
- [43] J. C. Slonczewski, Current-driven excitation of magnetic multilayers, *J. Magn. Magn. Matter* **159**, L1 (1996).
- [44] S. Zhang, P. M. Levy, and A. Fert, Mechanisms of spin-polarized current-driven magnetization switching, *Phys. Rev. Lett.* **88**, 236601 (2002).
- [45] A. Brataas, A. D. Kent, and H. Ohno, Current-induced torques in magnetic materials, *Nat. Mater.* **11**, 372 (2012).
- [46] D. Ralph and M. Stiles, Spin transfer torques, *J. Magn. Magn. Matter.* **320**, 1190 (2008).
- [47] R. Cheng, M. W. Daniels, J.-G. Zhu, and D. Xiao, Ultrafast switching of antiferromagnets via spin-transfer torque, *Phys. Rev. B* **91**, 064423 (2015).
- [48] R. Glaum and R. Gruehn, Synthese, Kristallstruktur und magnetisches Verhalten von V<sub>2</sub>PO<sub>5</sub>, *Z. Kristallogr.* **186**, 91 (1989).
- [49] E. Pachoud, J. Cumby, C. T. Lithgow, and J. P. Attfield, Charge Order and Negative Thermal Expansion in V<sub>2</sub>OPO<sub>4</sub>, *J. Am. Chem. Soc.* **140**, 636 (2018).
- [50] B. Ech-Chahed, F. Jeannot, B. Malaman, and C. Gleitzer, Préparation et étude d'une variété basse température de l'oxyphosphate de fer de valence mixte  $\beta$ Fe<sub>2</sub>(PO<sub>4</sub>)O et de NiCr(PO<sub>4</sub>)O: Un cas d'échange électronique rapide, *J. Solid State Chem.* **74**, 47 (1988).